5. Lehninger, A. L.; Nelson, D. L.; Cox, M. M. *Principles of Biochemistry*; 2nd ed.; Worth Publishers: New York, 1993; (a) pp 642-649. (b) p 458.
6. (a) Briggman, B.; Oskarsson, Å. *Acta Crystallogr.* **1977**, *B33*, 1900. (b) Gottschalk, K. E.; Hiskey, R. G.; Pedersen, L. G.; Koehler, K. A. *J. Mol. Struct. (Theochem)* **1981**, *76*, 197.
7. (a) Goedkoop, J. A.; MacGillavry, C. H. *Acta Crystallogr.* **1957**, *10*, 125. (b) Ajò, D.; Fragalà, I.; Granozzi, G.; Tondello, E. *J. Mol. Struct.* **1977**, *38*, 245. (c) Merchan, M.; Tomá, F.; Nebot-Gil, I. *J. Mol. Struct. (Theochem)* **1984**, *109*, 51.
8. (a) Sime, J. G.; Speakman, J. C.; Parthasarathy, R. *J. Chem. Soc.* **1970**, *A*, 1919. (b) Rao, S. N.; Parthasarathy, R. *J. Chem. Soc., Perkin Trans. 2* **1974**, *6*, 683. (c) Chapuis, G.; Zalkin, A.; Templeton, D. H. *J. Chem. Phys.* **1975**, *62*, 4919. (d) Briggman, B.; Oskarsson, Å. *Acta Crystallogr.* **1978**, *B34*, 3357. (e) Djinović, K.; Golič, L.; Hadži, D.; Orel, B. *Croat. Chim. Acta* **1988**, *61*, 405. (f) Djinović, K.; Golič, L.; Leban, I. *Acta Crystallogr.* **1990**, *C46*, 281. (g) Chapman, D.; Lloyd, D. R.; Prince, R. H. *J. Chem. Soc.* **1964**, 550. (h) Maury, L.; Bardet, L. *J. Raman Spectrosc.* **1978**, *7*, 197. (i) Gelb, R. I.; Schwartz, L. M.; Laufer, D. A. *J. Am. Chem. Soc.* **1981**, *103*, 5664. (j) Kidric, J.; Mavri, J.; Podobnik, M.; Hadži, D. *J. Mol. Struct.* **1990**, *237*, 265. (k) Mavri, J.; Hodoscek, M.; Hadži, D. *J. Mol. Struct. (Theochem)* **1990**, *209*, 421.
9. McDaniel, D. H.; Brown, H. C. *Science* **1953**, *118*, 370.
10. Adachi, M.; Nakagawa, J.; Hayashi, M. *J. Mol. Spectrosc.* **1982**, *91*, 381.
11. Stewart, J. J. P. MOPAC version 6.0, QCPE Program No. 455, Indiana University, Bloomington, IN.
12. (a) Kang, Y. K.; Némethy, G.; Scheraga, H. A. *J. Phys. Chem.* **1987**, *91*, 4105. (b) Kang, Y. K.; Némethy, G.; Scheraga, H. A. *J. Phys. Chem.* **1987**, *91*, 4109. (c) Kang, Y. K.; Némethy, G.; Scheraga, H. A. *J. Phys. Chem.* **1987**, *91*, 4118. (d) Kang, Y. K.; Gibson, K. D.; Némethy, G.; Scheraga, H. A. *J. Phys. Chem.* **1988**, *92*, 4739.

Synthesis, Structural and Electrical Characterizations of $Pr_{2-x}Ba_xNiO_{4\pm\delta}$[§]

Young Kee Chung, Young-Uk Kwon*, and Song Ho Byeon†

Department of Chemistry, Sung Kyun Kwan University, Suwon 440-746, Korea
†Department of Chemistry, Kyung Hee University, Yong-In, 449-701, Korea
Received September 15, 1994

Solid solutions of $Pr_{2-x}Ba_xNiO_{4\pm\delta}$ with K_2NiF_4-type structure were prepared in air and characterized by powder X-ray diffraction, Rietveld refinements, iodometry titrations, and conductivity measurements. The range of the solid solution was $0\leq x<0.5$. The crystal structure changes from orthorhombic (Fmmm) for $x\leq 0.1$ to pseudo-tetragonal ($I4/mmm$) for $x\geq 0.2$. The orthorhombic structure of $x=0.1$ transforms to tetragonal at low temperature. The bond distances obtained from the Rietveld analyses did not vary significantly with the Ba content except that of Ni-O (parallel to the *c*-axis) which showed an abrupt increase from $x=0.1$ to 0.2. The excess oxygen content (δ) decreases from 0.241 to 0.03 with increasing substituted Ba contents within the solution range. The samples are all semiconductors at the temperature range $4<T<300$ K.

Introduction

There has been a considerable effort to the study of $Ln_{2-x}A_xNiO_4$ (Ln: rare earths, A: alkaline earths) in both synthesis and structural characterizations.[1-4] These materials have attracted interest because of their close relationship to the superconducting $Ln_{2-x}A_xCuO_4$ phases.[5] Furthermore, the reported metal-insulator transitions in $La_{2-x}Sr_xNiO_4$[2] and the anisotropic physical properties of La_2NiO_4[3,4] prompted many research groups to investigate related $Ln_{2-x}A_xNiO_4$ systems. Besides the interesting metal-insulator transitions as a function of the amount of alkaline earths substitution (x) and/or temperature, there are very intriguing questions to the structure and composition. The ideal tetragonal ($I4/mmm$) K_2NiF_4 (or A_2BO_4) structure (Figure 1) can be slightly modified into Fmmm, Pccn, Bmab, $P4_2/ncm$ phases depending on the nature of the rare earth, the alkaline earth, degree of substitution (x), and the amount of excess interstitial oxygen (δ). Table 1 summarizes the reported results on the solid solutions of $Ln_{2-x}A_xNiO_{4\pm\delta}$ phases for their solid solution ranges and structures. It is noticeable that among the alkaline earths strontium is the most effective in forming solid solutions and is the only one that can stabilize the K_2NiF_4-type structures with Sm,[8] Gd,[8] and Y[12] which themselves alone cannot even form nickelates in this structure type.

Unsubstituted $Pr_2NiO_{4\pm\delta}$ has variable structures depending on the amount of the interstitial oxygen (δ). The structure is in the space group Fmmm for $\delta>0.20$,[13] $P4_2/ncm$ for $\delta=$

[§]This paper is dedicated to professor Woon-Sun Ahn in honor of his retirement.
*To whom correspondence should be addressed.

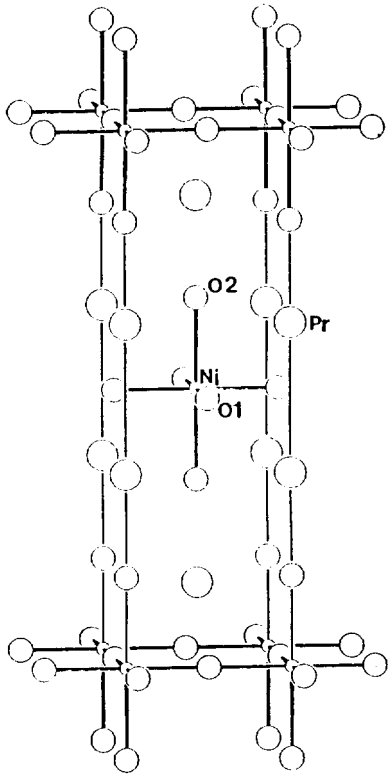

Figure 1. Ideal tetragonal structure and atom labels for Pr_2NiO_4.

0.060, and Pccn for $\delta=0.020$ at high temperature. When the $\delta=0.020$ sample was cooled below 118 K, there were both the orthorhombic and tetragonal phases.[14] $Nd_2NiO_{4\pm\delta}$ shows a structural transition from Bmab to Fmmm at $\delta=0.13$. The structures found for $La_2NiO_{4\pm\delta}$ were Bmab ($\delta=0.0$-0.007), $P4_2/ncm$ ($\delta=0.02$-0.03), $I4/mmm$ ($\delta=0.168$-0.18), and Fmmm ($\delta=0.25$).[15] Between the δ-regions listed above are biphasic regions. Even though the ionic radii of La (1.36 Å), Pr (1.32 Å), and Nd (1.30 Å) are very close to one another, their nickelate compounds behave much differently but still in somehow related manner. These examples demonstrate the complex nature of the system that prohibits any simple-minded generalizations and conjecture of one system from the other.

The solid solutions $Nd_{2-x}A_xNiO_{4\pm\delta}$ (A=Ca, Sr, and Ba) show structure variations with the alkaline earth substitution.[9-11] Takeda *et al.* studied these series of compounds synthesized with controlled oxygen contents close to ideal $\delta=0$.[10] At low x, the structure was Bmab, the same as the unsubstituted Nd_2NiO_4. Sr and Ba substitutions turn the structure into $I4$ /mmm from $x=0.2$ and 0.1, respectively, while Ca substitution results in Fmmm structure from $x=0.4$. Greenblatt and her group reported different results on the same system. They reported orthorhombic phase for Ca and Ba substituted cases all over the solution ranges. The reported a and b lattice parameters of the Ba containing phases approach to each other and become statistically indistinguishable from $x=0.2$ and thereafter. Yet, they still assigned these seemingly tetragonal phases as orthorhombic based on the line splitting of their Guinner powder patterns at high angles. In other paper, they reported tetragonal structure for Sr substituted

Table 1. Summary of literature results for the composition and the structure of solid solution $Ln_{2-x}A_xNiO_4$ (Ln; La, Pr, Nd, Sm, Gd, Y, A; Ca, Sr, Ba)

Ln \ A	Ca	Sr	Ba
La		1. $0\le x\le 1.6$ 2. 3. 4. 2, 6	1. $0\le x\le 1$ 2. T[a] 3. 4. 7
Pr		1. $0\le x\le 1$ 2. O $x<0.2$ T $x\ge 0.2$ 3. 4. 8	1. $0\le x\le 0.4$ 2. Fmmm $x<0.2$ $I4/mmm$ $x\ge 0.2$ 3. Rietveld analysis 4. this work
Nd	1. $0\le x\le 0.6$ 2. Bmab $x<0.4$ Fmmm $x\ge 0.4$ 3. Rietveld analysis 4. 9, 10	1. $0\le x\le 1.4$ 2. Bmab $x<0.2$ $I4/mmm$ $x\ge 0.2$ 3. Rietveld analysis 4. 9, 11	1. $0\le x\le 0.6$ 2. $I4/mmm$ 3. Rietveld analysis 4. 9, 10
Sm		1. $0.5\le x\le 1$ 2. O $x<0.8$ T $x\ge 0.8$ 3. 4. 8	
Gd		1. $x=1$ 2. 3. fixed composition 4. 8	
Y		1. $x=1.67$ 2. $I4/mmm$ 3. fixed composition of $YSr_5Ni_3O_{11}$ 4. 12	

*1) the solid solution range (x), 2) the crystal structure or the space group, 3) some remarks, 4) reference data for solid solution $Ln_{2-x}A_xNiO_4$ are summarized. The results for alkaline-earth free samples are not included. [a]abbreviations; O: orthorhombic, T: tetragonal.

phase with $0.2<x<0.8$. Only obvious difference between these contradicting results from the two research groups is the oxygen content. Therefore, it seems very important to study the structural dependency of the $Ln_{2-x}A_xNiO_{4\pm\delta}$ system both on the A substitution and excess oxygen content.

We have noticed that Pr containing system has been studied only for A=Sr.[8] This system showed much similarity to that of Nd analogue without oxygen control in both structure and physical properties. In order to get a general view, we have started the investigations for the $Pr_{2-x}A_xNiO_{4\pm\delta}$ systems with A=Ca and Ba. In this paper, we will present our results on the solid solution of $Pr_{2-x}Ba_xNiO_{4\pm\delta}$ for the synthesis, structural characterizations through Rietveld refinements, and transport properties.

Table 2. Lattice parameters, space groups, and the oxygen content in $Pr_{2-x}Ba_xNiO_{4\pm\delta}$

x	Space Group	Unit cell parameter (Å)			Unit cell volume (Å^3)	Oxygen Content (δ)
		a	b	c		
0.0	Fmmm	5.4612(8) 3.8313(8)[a]	5.3964(8)	12.456(2)	183.55(7)[b]	0.241(6)
0.1	Fmmm	5.4430(9) 3.8355(8)[a]	5.4037(7)	12.513(2)	184.02(7)[b]	0.18(1)
0.2	*I*4/mmm	3.8307(4)		12.563(2)	184.34(3)	0.137(6)
0.3	*I*4/mmm	3.8281(2)		12.600(1)	184.65(2)	0.094(8)
0.4	*I*4/mmm	3.8263(3)		12.653(1)	185.25(3)	0.03(2)

[a] a-parameter for the corresponding tetragonal cell obtained with the following equation: $a_t=(a_o+b_o)/2\sqrt{2}$, where a and b stand for the lattice parameters t and o for the tetragonal and orthorhombic structures, respectively. [b] Reduced unit cell volume to those of the tetragonal cell.

Experimental

Samples of $Pr_{2-x}Ba_xNiO_{4\pm\delta}$ ($0\le x\le 0.7$) compositions were prepared by co-decomposition of the metal nitrates. Stoichiometric quantities of $Pr(NO_3)_3\cdot 6H_2O$ (Aldrich, 99.9%), $Ba(NO_3)_2$ (Aldrich, 99+%), $Ni(NO_3)_2\cdot 6H_2O$ (JANSSEN, 99%) were decomposed in crucibles by torch flame and the resulting solids were calcined in air at 900 ℃ for 15 hr. These powder samples were ground in agate mortar and made into pellets, and heated in air at 1300 ℃ for 200 hr in Pt-boats with intermittent grindings. In order to see the effect of temperature, reactions at 1200 ℃ and 1400 ℃ were also performed in the similar manner. The samples were slow cooled in the furnace to room temperature. Powder X-ray diffraction (XRD) data, collected on a Rigaku diffractometer with monochromatized CuKα radiation were used to monitor the progress of the reactions. Least-squares refinement of the observed 2θ values was used in the evaluation of the lattice parameters.

The total oxygen content was determined by iodometric titration. For iodometric titration, a sample (about 30-40 mg) and KI (2 g) were dissolved in distilled water with 6 N-HCl (4 mL), and diluted in 30 mL-distilled water. The solution was titrated with a standardized thiosulfate solution under N_2 atmosphere. A few drops of a 5% starch solution were added just before the equivalence point as an indicator. The oxygen contents (δ) in Table 2 and in the following text are averaged values from three or four such titrations for each sample.

Rietveld refinements[16] were performed for the samples from the 1300 ℃ reactions. MacScience diffractometer running with current 0.3 Amp and 50 kV was utilized. The intensity data were obtained with step size 0.02° in 2θ, and the scan time 1 sec over 2θ range 20°-120°. DBWS-9006PC[17] program was used for the profile refinement. The systematic absence found in the powder pattern suggested space groups *I*4/mmm or Fmmm. The choice between these was based on the splitting of *hk*0 peaks. The $x=0.0$ and 0.1 data showed such splitting and were refined in Fmmm space group. The rest of data were refined in both Fmmm and *I*4/mmm. The refinement conditions and restrictions are as follows: a pseudo-Voigt function for the peak profile and the mixing parameters of Gaussian and Lorentzian contributions were refined, each peak profile was refined within the range 10 times in 2θ of the full-width-of-half-maximum, asymmetric correction was included for the peak shape up to $2\theta=90°$, and the sample displacement parameter was refined while the zero-error was fixed at null.[18]

Conductivity measurements were carried out with a standard four-probe technique with silver wire and silver paste contact at temperature range of 10-310 K.

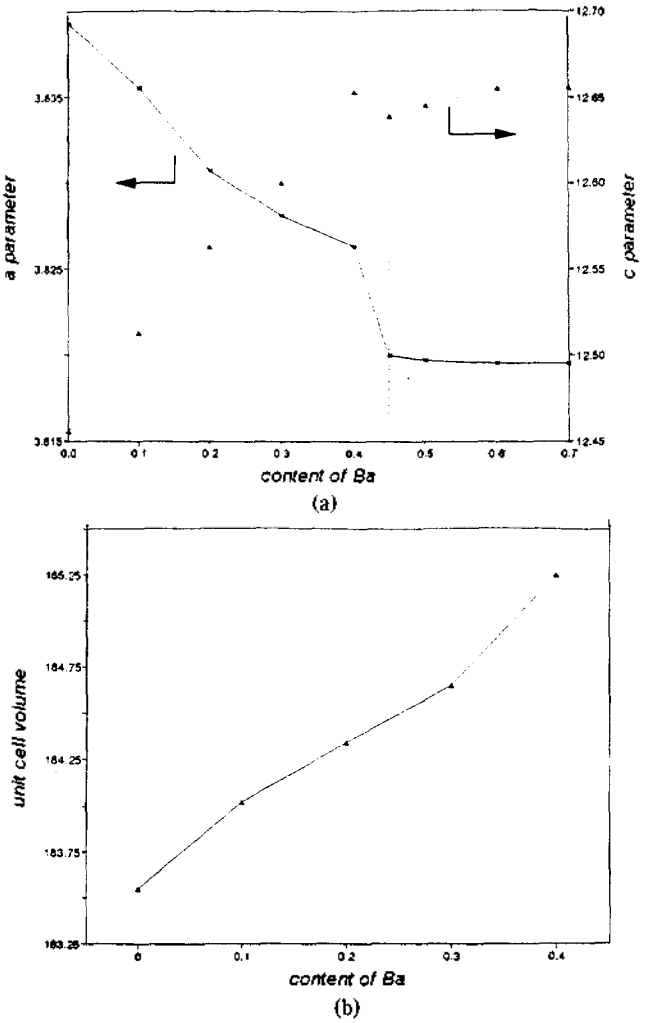

Figure 2. The variations of a) a- and c-parameters, and b) unit cell volume as a function of the Ba content (x) of $Pr_{2-x}Ba_xNiO_{4\pm\delta}$. Data points for $x<0.5$ are for sample obtained from 1300 ℃ reaction and the rest are from 1200 ℃.

Results and Discussion

Synthesis. Single phase products in the $Pr_{2-x}Ba_xNiO_{4\pm\delta}$ solid solution were synthesized up to $x=0.4$ at between 1200 ℃ and 1300 ℃ and to $x=0.5$ at 1400 ℃, as evident from the powder diffraction patterns (Table 2). As more Ba was present in the sample than the limit, there were found $BaPrO_3$ and NiO as impurities. The extrapolations of the lattice parameters from the solid solution and the saturation regions

for both a and c parameters meet at around $x=0.45$ (see Fig. 2). We understand that this is the achievable solubility limit which may not be possible due to kinetics of diffusion. Therefore, it appears that the larger x_{max} obtained from the 1400 ℃ synthesis is a mere consequence of the higher mobility of atoms and faster equilibration at higher temperature.

This rather limited solid solution range for Ba substitution is also found in the Nd-analogues with $x_{max}=0.5$.[9,10] The La-analogue is reported to have $x_{max}=1.0$[7]. This contrasts very sharply with the much larger x_{max} values for the Sr substitution cases in the La, Pr, and Nd-based nickelates up to $x=1.6$.[8,10,11]

When discussing the stability for the K_2NiF_4-type compound, the tolerance factor (t_k) argument is often employed.[20] The tolerance factor is defined as $t_k=(r_A+r_O)/\sqrt{2}(r_B+r_O)$ where r's are ionic radii of atoms at the crystallographic sites for the general formula A_2BO_4. Yokokawa, *et al.* discussed that the K_2NiF_4-type structure is found for $0.85<t_k<1$ and that for t_k close to 1 the ideal tetragonal structure is preferred.[21] With rare earths alone, the tolerance factors of the nickelates are 0.89 for La, 0.87 for Pr, and 0.87 for Nd-based compounds. Sr or Ba substitutions for the rare earths will give larger t_k values of Ln_2NiO_4 because of the larger atomic radii of Sr (1.45 Å) and Ba (1.61 Å) than those of Ln (1.36 Å-1.21 Å) and thus higher stability for the K_2NiF_4-structure. Especially, Ba would have the strongest effect to stabilize the structure with the tolerance factor close to one.

The reported narrower solution range for Ca substitutions in Nd-based nickelates with 0.6[10] than for Sr can be understood with this tolerance factor arguments: Ca is smaller than Ln resulting in even smaller t_k and thus the K_2NiF_4 structure is destabilized rapidly with added Ca. However, the foregoing discussion fails to explain why solubility range for Ba is much smaller than that of Sr substitution in Ln_2NiO_4 (Ln=pr, Nd). The tolerance factor argument is only phenomenological and does not have a firm theoretical foundation. Moreover, it is only applicable to the average of the structure. We would like to argue that the limited solid solubility for the Ba substitution was originated from the large size difference between Ba and Ln. In metallurgy, a rule of thumb for a complete solid solution alloy is that the constituting elements should not have a size difference larger than 15%.[22] With larger size differences, the alloy lattice is heavily distorted which is thermodynamically unfavorable. When Ba is introduced to the lattice of Ln_2NiO_4, the lattice will experience tension because Ba requires larger space than the rest of the structure can provide. Such tension is partly reflected on the expansion of the lattice (vide infra). However, this is an averaged result over the whole sample. The very site where Ba and Ln are neighboring to each other will still have a high degree of tension. Somehow the lattice absorbs this destabilizing effect in such mechanisms as lattice expansion and microscopic distortions. Such mechanisms seem to more than offset the tension arising from Sr substitutions all over the compositions up to $x=1.6$.[9-11] However, Ba substitution gives rise to larger lattice tension for which the compensation can be effective only for limited range. The fact that the $La_{2-x}Ba_xNiO_4$ system has larger solubility range up to $x=1.0$ than the Pr- or Nd-analogues partly support this argument. Even though the present oxide case has many different features from those of alloys, the microscopic distortion argument due to the size difference between Ln and Ba seems valid to explain the small solid solubilities of Ba containing systems.

The oxygen content (δ) decreases monotonically from 0.241 ($x=0.0$) to 0.03 ($x=0.4$) with increasing Ba content. $Nd_{2-x}Ba_xNiO_{4\pm\delta}$ synthesized in air shows almost identical trend.[9] Calculated portions of Ni^{3+} for these samples are nearly constant at 47% regardless the Ba content. This indicates that the oxidation state of nickel is determined largely by the oxygen potential of the reaction atmosphere rather than by the structural requirement. The excess oxygen is reported to be interstitial ones at (0.25, 0.25, 0.25) position of the orthorhombic lattice.[23]

Structure. The refined lattice parameters were plotted in Figure 2. The orthorhombic a and b parameter values for $x\leq0.1$ data were transformed into corresponding tetragonal one for comparison. The tetragonal a-parameter monotonically decreases and the c-parameter increases with the Ba content up to slightly beyond the solution range and then are saturated. The unit cell volume monotonically increases with increasing Ba content. The same trends are found in the analogous La or Nd containing systems. The $La_{2-x}Ba_xNiO_4$ system, which has wider x range shows upturn for a parameter at $x=0.5$ and downturn for c at $x=0.6$. Because of small x_{max} in our system, such up- and downturns did not appear. There are some factors that can contribute to the unit cell size change. Firstly, the oxidation of Ni from 2+ to 3+ upon Ba substitution and concurrent decrease of atomic size from $r_{Ni^{2+}}=0.83$ Å to $r_{Ni^{3+}}=0.70$ Å (low spin) or 0.74 Å (high spin) can shrink the cell. Secondly, the reducing amount of interstitial oxygen with incresing x value can also compress the cell. Thirdly, the larger size of Ba than Ln induces unit cell expansion. The characteristic lattice parameter variation with the alkaline earth substitution in each system of $Ln_{2-x}A_xNiO_4$ must be a result of a subtle balance of factors discussed above and from other sources. Apparently, the last effect overwhelms the other in the range $0.1<x<0.5$ but not in $x<0.1$ region in the present case and other A=Ba case.

The orthorhombic distortion of the K_2NiF_4-structure manifests itself by the splitting of some the *hk*0-type reflections in the powder x-ray diffraction pattern. The degree of divergence is the degree of distortion from the ideal tetragonal geometry. Splitting of the *hk*0 peaks in the powder x-ray diffraction of $Pr_{2-x}Ba_xNiO_{4+\delta}$ was observed for $x\leq0.2$. These split peaks merge in higher Ba cases and the powder patterns appear to be those of tetragonal for $x\geq0.2$. Similar orthorhombic to tetragonal transition was found in $Nd_{2-x}Ba_xNiO_4$ system.[9] The transition appeared to occur at $x=0.2$ as judged from the reported lattice parameters. La-containing system, however, has tetragonal phases only all over the solution range. In these cases the tolerance factors seem to correlate with structures very well. Unsubstituted Pr and Nd compounds have tolerance factors (0.87 for both cases) close to the lowest limit, 0.85, for the K_2NiF_4-type structure and, therefore, a distorted lattice is expected which is in accordance to the reported orthorhombic Fmmm structure. As Sr or Ba substitute the rare earths, the tolerance factor grows and the undistorted tetragonal lattice appears. In the $La_{2-x}A_xNiO_4$ case, La is larger than Pr and Nd and the tolerance factor is large (0.89) even without A substitution and, thus, the undistorted tetragonal structure is stable all over

Table 3. Crystal data from the Rietveld refinements of $Pr_{2-x}Ba_xNiO_{4\pm\delta}$

x		0.1	0.1	0.2[a]		0.3[a]		0.4[a]	
Space Group		Fmmm	Fmmm	*I*4/mmm	Fmmm	*I*4/mmm	Fmmm	*I*4/mmm	Fmmm
unit cell	a	5.45670(9)	5.43750(7)	3.82836(3)	5.41575(9)	3.82643(3)	5.4100(1)	3.82413(3)	5.4067(1)
parameter	b	5.39292(9)	5.39994(7)		5.41240(9)		5.4128(1)		5.4098(1)
(Å)	c	12.4464(2)	12.5008(2)	12.5562(1)	12.5561(1)	12.5942(1)	12.5942(1)	12.6443(2)	12.6443(2)
atomic	Pr/Ba, z	0.3591(1)	0.3601(1)	0.3601(1)	0.3601(1)	0.3605(1)	0.3605(1)	0.3614(1)	0.3614(1)
position[b]	O(2), z	0.169(1)	0.1686(9)	0.1738(9)	0.1738(9)	0.172(1)	0.172(1)	0.173(1)	0.172(1)
isotropic	Pr/Ba	1.42(3)	1.37(2)	1.17(2)	1.18(2)	1.16(2)	1.17(2)	1.07(2)	1.06(2)
thermal	Ni	1.41(7)	1.43(7)	1.56(7)	1.56(7)	1.41(7)	1.42(7)	1.26(7)	1.24(7)
parameter	O(1)	3.5(3)	5.1(3)	4.3(3)	4.3(3)	2.9(3)	2.9(3)	2.6(3)	2.6(3)
	O(2)	4.3(3)	4.4(3)	3.5(3)	3.5(3)	4.0(3)	4.0(3)	2.4(2)	2.4(2)
R_B[c]		7.22	6.45	7.80	7.81	8.53	8.56	9.48	9.38
R_F[c]		5.82	4.85	5.44	5.36	5.62	5.53	6.35	6.29
R_P[c]		12.22	11.93	12.60	12.42	12.64	12.62	13.89	14.00
R_{WP}[c]		17.02	16.20	17.24	17.08	17.07	17.02	18.70	18.72

[a] refinement results for both orthorhombic and tetragonal structures of $x=0.2$-0.4 samples are given for comparison (see text). [b] general positions: 0, 0, z (0, 0, z) for Pr/Ba and O(2), 0, 0, 0 (0, 0, 0) for Ni, and 0, 1/2, 0 (1/4, 1/4, 0) for O(1) in *I*4/mmm (in Fmmm). [c] $R_B=\frac{\Sigma|I_{obs}-I_{calc}|}{\Sigma|I_{obs}|}$, $R_F=\frac{\Sigma||F_{obs}|-|F_{calc}||}{\Sigma|F_{obs}|}$, $R_P=\frac{\Sigma|Y_{io}-Y_{ic}|}{\Sigma Y_{io}}$, $R_{WP}=\left[\frac{\Sigma w_i(Y_{io}-Y_{ic})^2}{\Sigma w_i Y_{io}}\right]^{1/2}$.

the solubility range.

The Rietveld refinement results are summarized in Table 3. The refinements were conducted with the Fmmm model for $x=0.0$ and 0.1 and with both the Fmmm and *I*4/mmm models for $x\geq0.2$ data. The first two samples showed clear peak splittings of *hk*0, characteristic of orthorhombic distortion. For the rest of seemingly tetragonal phases, it was still possible to have incomplete peak splittings, that is, line broadening of *hk*0. Rietveld profile fitting appeared to be well suited to resolve such problems. Note that the only difference between *I*4/mmm and Fmmm is the additional *b*-parameter for the latter; there is no such distortion as tilting or atom displacement in the *I*4/mmm to Fmmm transition. Theoretically, including this additional parameter in the refinement should result in a better fit. Refinements for $x\geq0.2$ samples in Fmmm model resulted in slightly different *a* and *b* parameters but practically the same agreement factors (R-indices) indicating that there is no significant peak broadening at all (Table 3). Therefore, it is concluded that the orthorhombic to tetragonal transformation in $Pr_{2-x}Ba_xNiO_4$ occurs at $0.1<x<0.2$.

The important bond distances from the refinements are listed in Table 4 and are plotted in Figure 3. There is no noticeable variations of the bond distances except that of Ni-O(2). The axial Ni-O(2) bond in the NiO_6 octahedron shows a step jump by about 0.07 Å between the orthorhombic and tetragonal regimes. The origin for the jump is not clear as yet but may be related to the presence of interstitial oxygens. According to our titration results, larger amount of excess oxygens are present in the orthorhombic than in the tetragonal samples. The interstitial oxygens are located inbetween two parallel to the ab-plane Pr-O(2) layers. These interstitial oxygens will repel neighboring negatively charged oxygens, O(2), toward Ni resulting in short Ni-O(2) distances.

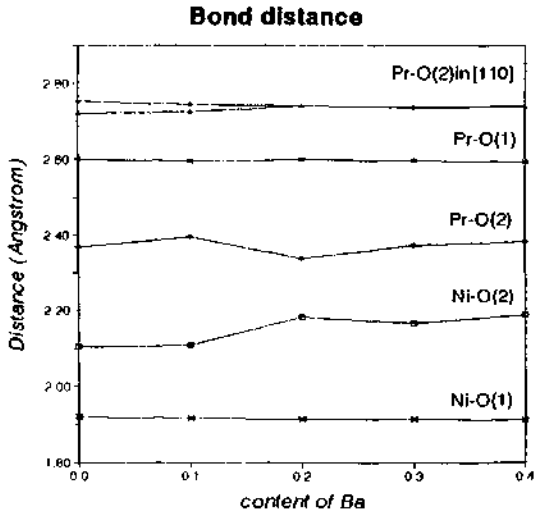

Figure 3. Variations of Ni-O and Pr(Ba)-O bond distances in the $Pr_{2-x}Ba_xNiO_4$ system.

Our results contrast those for $Nd_{2-x}A_xNiO_4$ (A=Ca, Sr, and Ba) with nearly stoichiometric oxygen content in the bond distance trends.[16] In the system, the bond distances and their changes with x did not show any significant dependence on the nature of A. The Ni-O distances and Pr/A-O(1) remained unchanged up to $x=0.5$, but the Nd/A-O(2) parallel to the c-axis gradually increases and the Nd/A-O(2) in [110] direction decreases with x. One of the reasons for the different bond distance trends between our system and $Nd_{2-x}A_xNiO_4$ is the different oxygen content. However, it is not clear what makes these similar systems show such distinctions.

A Rietveld refinement of the low temperature (10 K) pow-

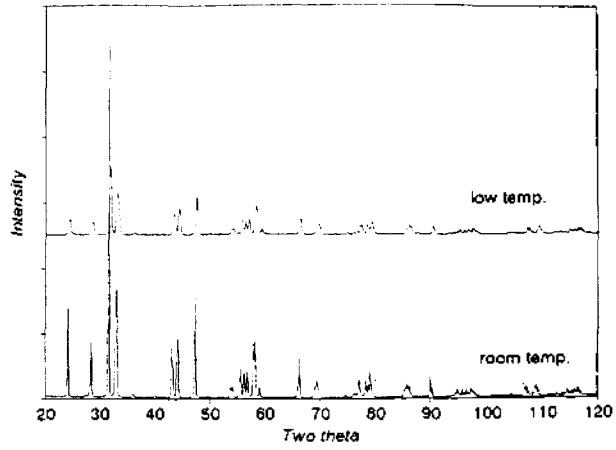

Figure 4. X-ray powder patterns of $Pr_{1.9}Ba_{0.1}NiO_{4\pm\delta}$ at 300 K (lower curve) and 10 K (upper curve).

der pattern for the $x=0.1$ sample was attempted in order to see any structural changes. However, because of the low quality of the data no acceptable refinement result was obtained. Nonetheless, the powder pattern (Figure 4) clearly shows that the low temperature structure is tetragonal with merged *hk*0 peaks. Closely related $Pr_2NiO_{4.020}$ is reported to be orthorhombic (Pccn) at room temperature and undergoes a structural transformation to tetragona ($P4_2/ncm$) below 118 K.[14]

Conductivity. The resistivity measurement conducted in the temperature range 10 to 310 K showed a characteristic behavior of semiconductor for all the samples. There is not much variation from one sample to the other in the conductivity *vs.* temperature curves. Similar $Nd_{2-x}A_xNiO_{4\pm\delta}$ (A=Ca, Sr, Ba) and $Pr_{2-x}Sr_xNiO_{4\pm\delta}$ systems were reported to be semiconducting also. Contrarily, when the oxygen content was controlled to nearly stoichiometric, the $Ln_{2-x}Sr_xNiO_4$ (Ln=La,[6] Nd[10]) systems showed a metal to semiconductor transitions with the transition temperature decreased monotonically with increasing Sr content. Such transition have been understood in terms of band gap closing[6] or increased hole concentration with Sr amount, but still remain controversial. The portion of the Ni^{3+} seems to be important for the electric property. Also the interstitial oxygen and possibly the oxygen defect in the Ni-O network seem to play a detrimental role by trapping the charge carrier as is seen in our and other oxygen excess systems.

In conclusion, we have synthesized solid solution $Pr_{2-x}Ba_xNiO_{4\pm\delta}$ in the K_2NiF_4-type structure. The structure changed from orthorhombic to tetragonal with the Ba content increase. These samples showed semiconducting behavior at temperature between 10 to 310 K. There are many aspects of this system that are not fully understood. We are going to study this system further for the low temperature structure and conductivity on the oxygen controlled samples as well as magnetic properties.

Acknowledgment. Financial support from the Ministry of Education through the Basic Sience Research Program, BSRI-94-3421, is gratefully thanked.

References

1. Takeda, Y.; Kanno, R.; Sakano, M.; Yamamoto, M.; Takano, R.; Banndo, Y.; Akinaga, H.; Takita, K.; Goodenough, J. B. *Mater. Res. Bull.* **1990**, *25*, 293.
2. Gopalakrishinan, J.; Colsmann, G.; Reuter, B. *J. Solid State Chem.* **1977**, *22*, 145.
3. Rao, C. N. R..; Buttrey, D. J.; Otsuka, N.; Ganguly, P.; Harrison, H. R.; Sandberg, C. T.; Honig, J. M. *J. Solid State Chem.* **1984**, *51*, 266.
4. Buttrey, D. J.; Honig, J. M.; Rao, C. N. R. *J. Solid State Chem.* **1986**, *64*, 287.
5. Bednorz, J. G.; Muller, K. A. *Z. Phys.* B. **1986**, *64*, 189.
6. Granados, X.; Fontcuberta, J.; Valler-Regi, M.; Sayagues, M. J.; Gonzalez-Calbet, J. M. *J. Solid State Chem.* **1993**, *102*, 455.
7. Austin, A. B.; Carreiro, L. G.; Marzik, J. V. *Mater. Res. Bull.* **1989**, *24*, 639.
8. Chen, S. C.; Ramanujachary, K. V.; Greenblatt, M. *J. Solid State Chem.* **1993**, *105*, 444.
9. Arbuckle, B. W.; Zhang, Z.; Greenblatt, M. *In Chemistry of Electronic Ceramic Materials*; Davis, P. K.; Roth, R. S., Eds.; NIST pub. 804; Washington: 1991, p 207.
10. Takeda, Y.; Nishijima, M.; Imanishi, N.; Kanno, R; Yamamoto, O. *J. Solid State Chem.* **1992**, *96*, 72.
11. Arbuckle, B. W.; Ramanujachary, K. V.; Zhang, Z.; Greenblatt, M. *J. Solid State Chem.* **1990**, *88*, 278.
12. James, M.; Attfield, J. P. *J. Solid State Chem.* **1993**, *105*, 287.
13. Saez-Puche, R.; Fernandez, F.; Glaunsinger, W. S. *Mater. Sci. Monogr. (React. Solu. Pt. A)* **1985**, *28*, 607.
14. Buttrey, D. J.; Sullivan, J. D.; Shirane, G.; Yamada, K. *Phys. Rev.* B **1990**, *42*, 3944.
15. Rice, D. E.; Buttrey, D. J. *J. Solid State Chem.* **1993**, *105*, 197.
16. Rietveld, H. M. *Acta Cryst.* **1967**, *22*, 151.
17. Sakthivel, A.; Young, R. A. User's guide to programs DBWS-9006 and DBWS-9006PC for Rietveld analysis of X-ray and neutron powder diffraction patterns; Atlanta, GA: 1990.
18. Post, J. E.; Bish, D. L. *Reviews in Mineralogy* **1989**, *20*, 277.
19. DiCarlo, J.; Mehta, A.; Banschick, D.; Navrotsky, A. *J. Solid State Chem.* **1993**, *103*, 186.
20. Yokokawa, H.; Kawada, T.; Dokiya, M. *J. Am. Ceram. Soc.* **1989**, *72*, 152.
21. Yokokawa, H.; Sakai, N.; Kawada, T.; Dokiya, M. J. *Solid State Chem.* **1991**, *94*, 106.
22. Evans, R. C. *An introduction to crystal chemistry*; 2nd Ed.; Cambridge: University Press: Cambridge, U. K., 1966; p 311.
23. Jorgensen, J. D.; Dabrowski, B.; Pei, S.; Richards, D. R.; Hinks, D. G. *Phys. Rev.* B. **1989**, *40*, 2187.